Article:
Park, JH, Waickman, AT, Reynolds, J et al. (2 more authors) (2019) IL7 receptor signalling in T cells: a mathematical modelling perspective. Wires Systems Biology and Medicine, 11 (5). e1447. ISSN 1939-5094

https://doi.org/10.1002/wsbm.1447

IL7 receptor signalling in T cells: a mathematical modelling perspective

Jung-Hyun Park[1], Adam T. Waickman[1], Joseph Reynolds[2], Mario Castro[3,4] and Carmen Molina-París[4]
[1] Experimental Immunology Branch, National Cancer Institute, NIH, Bethesda, MD, USA.
[2] Safety and environmental assurance centre (SEAC), Unilever, UK.
[3] Universidad Pontificia Comillas, GISC and DNL, Madrid, Spain.
[4] Department of Applied Mathematics, School of Mathematics, University of Leeds, Leeds, UK.

December 12, 2018

Abstract

Interleukin-7 (IL7) plays a non-redundant role in T cell survival and homeostasis, which is illustrated in the severe T cell lymphopenia of IL7-deficient mice, or demonstrated in animals or humans that lack expression of either the IL7Rα or γ_c chain, the two subunits that constitute the functional IL7 receptor. Remarkably, IL7 is not expressed by T cells themselves, but produced in limited amounts by radio-resistant stromal cells. Thus, T cells need to constantly compete for IL7 to survive. How T cells maintain homeostasis and further maximise the size of the peripheral T cell pool in face of such competition are important questions that have fascinated both immunologists and mathematicians for a long time. Exceptionally, IL7 down-regulates expression of its own receptor, so that IL7-signalled T cells do not consume extra-cellular IL7, and thus, the remaining extra-cellular IL7 can be shared among unsignalled T cells. Such an altruistic behaviour of the IL7Rα chain is quite unique between members of the γ_c cytokine receptor family. However, the consequences of this altruistic signalling behaviour at the molecular, single cell and population levels are less well understood and require further investigation. In this regard, mathematical modelling of how a limited resource can be shared, while maintaining the clonal diversity of the T cell pool, can help decipher the molecular or cellular mechanisms that regulate T cell homeostasis. Thus, the current review aims to provide a mathematical modelling perspective of IL7-dependent T cell homeostasis at the molecular, cellular and population levels, in the context of recent advances in our understanding of the IL7 biology.

1 Introduction

The IL7 receptor (IL7R) and its ligand, IL7, are essential and non-redundant drivers of T cell development and homeostasis [1, 2, 3, 4, 5, 6]. While T cells critically depend on IL7R signalling, IL7 itself is not expressed by T cells. Instead, IL7 is mostly expressed by stromal cells and non-T lineage lymphoid and myeloid cells [7], and the amount of IL7 production is considered to be developmentally set [8, 9]. Consequently, IL7 signalling at the single cell level is primarily controlled by IL7 receptor expression, and secondarily by IL7 availability in vivo. Thus, interrogating the molecular basis of IL7 receptor expression and regulation is important to understand the role of IL7 receptor signalling in T cell immunity.

The functional IL7 receptor is composed of the IL7-specific IL7Rα chain (CD127) and the common γ-chain (γ_c or CD132), which is shared with a series of other cytokines that include IL-2, IL-4, IL-9, IL15, and IL-21 [10]. Since γ_c expression is presumed to be constitutive and also found in significant amounts on all T cells [11], much of the past and current studies of IL7 signalling have been focused on the regulatory mechanisms of the IL7Rα chain. Notably, the IL7 receptor harbours many unique features that complicate the assessment of IL7R signalling and its downstream effects. Among others, IL7 receptor signalling down-regulates expression of its own receptor, so that IL7 signalling leads to suppression of further IL7R signalling [12]. Initiating such a negative regulatory feedback is quite unusual, because expression of most other members of the γ_c receptor family is up-regulated by their cognate cytokine signals [13]. Recent studies have shown that such unique behaviour profoundly affects the kinetics and magnitude of IL7 receptor signalling, and that this regulatory mechanism is essential to maintain normal T cell development and homeostasis [14, 12, 15]. In fact, IL7-induced down-regulation of IL7R prevents IL7 signalled T cells from further consumption of extra-cellular IL7, so that the limited amount of free IL7 can be shared among unsignalled T cells.

Such altruistic behaviour of the IL7R seems required to maximise the size and diversity of the peripheral T cell pool [12]. However, a greater understanding of the quantitative and qualitative immunological signalling effects, under continuous de-sensitisation and re-sensitisation of the IL7 receptor, requires stratification of the IL7 signalling components. We consider that assessing these issues at the molecular, single cell and population levels will benefit from mathematical modelling of this complex immune signalling pathway. Additionally, IL7Rα not only interacts with its ligand but also binds directly to γ_c proteins in the absence of IL7 [16, 17]. As a result, IL7Rα and γ_c can exist as a pre-associated, inactive receptor complex on the cell membrane, even prior to ligand engagement [16, 17]. Receptor pre-association brings in a couple of new variables into the circuitry of IL7R signalling. Since the γ_c chain is a shared component of multiple cytokines, pre-association of γ_c with IL7Rα would sequester the γ_c chain from association with other cytokine receptors, such as IL15Rβ, and could interfere with their signalling capability in trans. Moreover, IL7Rα/γ_c pre-association would change the IL7 binding affinity of IL7Rα, so that free IL7Rα proteins would have lower IL7 affinities than IL7Rα complexed with γ_c. Because on the cell surface the number of IL7Rα molecules is thought to vastly outnumber that of γ_c proteins [18], under such a scenario, there would be two different species of IL7Rα chains, *i.e.,* free and γ_c-complexed, on the cell surface. Significantly, the free form would be signalling-incompetent and could act as an IL7 scavenger. On the other hand, the γ_c pre-associated form would be signalling-competent, but outnumbered by un-associated IL7Rα proteins. How cellular exposure to IL7 would initiate signalling in cells that express a mixture of two distinct receptor species is an important question that could be addressed making use of the mathematical modelling methods presented in this review at the molecular, cellular and population scales (see Section 5.1).

Finally, enforced IL7 receptor expression does not promote, but paradoxically, inhibits both development and homeostasis of T cells [14, 15]. Whether this is due to excessive IL7 signalling on a per cell basis that would be detrimental for cell survival [15], or because of excessive IL7 consumption on a population basis, that would further limit IL7 availability [12], still needs to be clarified [19]. In addition, the IL7Rα chain has no intrinsic signalling capability and requires association with the tyrosine kinase JAK1, through its cytosolic tail, to trigger downstream signalling. But JAK1 proteins are unstable due to microRNA controlled post-transcriptional mechanisms, and this could potentially limit their availability for IL7Rα [20]. Thus, in addition to the extra-cellular events that control IL7 signalling at the level of receptor and ligand association, the roles of intra-cellular components in the IL7R signalling machinery must also be considered (see Section 5.1).

Collectively, interrogating how these unique aspects of IL7 receptor signalling are interweaved in the control of T cell development and homeostasis is essential to unravel the basic mechanisms that regulate T cell-mediated immune responses at both the single cell and population levels. Computational and mathematical models of the dynamical interactions between these many elements (immune molecules and cells)) have tremendously contributed to our understanding of cytokine receptor signalling [21, 22, 23, 18, 24, 25], and quantitative approaches and tools are also essential and required to dissect the contribution of individual nodes in the IL7 signalling pathway.

In this review, we highlight the current state of our knowledge of the basic IL7 receptor biology and focus on the role IL7 and IL7R have on mature CD8$^+$ T cells as drivers of survival and homeostasis. Furthermore, we document recent advances in the mathematical and computational modelling of IL7 receptor signalling and its application in furthering our understanding of the dynamics of immune receptor signalling at the molecular (see Section 5.1), cellular (see Section 5.2) and population levels (see Section 5.3).

2 IL7 receptor expression and function in T cell development and homeostasis

The signalling-competent IL7 receptor is a hetero-dimeric protein complex, composed of the specific IL7Rα chain and the γ_c receptor. In contrast to γ_c expression, IL7Rα expression is dynamically regulated during T cell development and differentiation, so that IL7Rα expression is the primary determinant of IL7 responsiveness [19]. During thymocyte development, IL7Rα is highly expressed on the most immature CD4, CD8$^+$ double-negative (DN) cells, but then terminated upon differentiation into CD4, CD8$^+$ double-positive (DP) cells [26, 27, 28]. IL7Rα signalling is required in immature DN cells to provide critical pro-survival and proliferative cues [1, 29]. However, continued IL7Rα expression on DP thymocytes is detrimental to T cell development, since it would interfere with selection of a T cell receptor (TCR)-dependent immunocompetent repertoire [14, 30]. The molecular mechanism that terminates IL7Rα protein expression and transcription on DP thymocytes is not known [31]. Interestingly, this feature is not evolutionary conserved, because DP thymocytes in humans express robust amounts of IL7Rα proteins [32]. Nonetheless, immature DP thymocytes in humans show dramatic down-regulation of γ_c protein expression, which

renders these cells IL7 unresponsive [32]. Thus, suppression of IL7R signalling in DP thymocytes is a common characteristic in both mice and humans, but that is achieved through different means.
TCR-induced positive selection results in re-expression of IL7Rα on both $CD4^+$ and $CD8^+$ lineage T cells [26]. Concomitant to IL7Rα upregulation, $CD8^+$ lineage committed thymocytes become IL7-responsive. $CD4^+$ lineage committed cells, on the other hand, remain IL7 unresponsive despite expressing large amounts of IL7Rα. In fact, it is the selective de-sensitisation of cytokine receptors in $CD4^+$ lineage cells that determines CD4/$CD8^+$ lineage choice in the thymus and imposes $CD4^+$ lineage choice [33]. Mechanistically, it was recently demonstrated that expression of the $CD4^+$ lineage-specific transcription factor ThPOK induces expression of Suppressor Of Cytokine Signalling (SOCS) genes, which in turn suppresses IL7R signalling to prevent up-regulation of the CD8-specifying transcription factor Runx3 [34]. Thus, surface IL7Rα expression does not necessarily guarantee productive IL7R signalling. Along this line, cytokine receptor de-sensitisation is another mechanism that needs to be considered to understand IL7 receptor signalling.
Multiple mechanisms have been proposed to induce de-sensitisation of IL7Rα signalling. Persistent TCR signalling that leads to destabilisation of IL7Rα-associated JAK1 expression, or up-regulation of SOCS1 expression to inhibit JAK kinase activity, and proteolytic cleavage of the γ_c chain cytosolic tail by the cysteine protease, calpain, are some of the proposed, and not necessarily mutually exclusive, mechanisms [35, 36, 20]. During thymocyte differentiation, regaining IL7 responsiveness is critical for $CD8^+$ single positive (SP) thymocyte generation because impaired IL7 signalling, either by enforced expression by SOCS1 or by conditional deletion of IL7Rα in pre-selection thymocytes, resulted in profoundly impaired generation of $CD8^+$ lineage cells [5, 27, 34]. The prerequisite for IL7 signalling in $CD8^+$ cells is mostly due to a STAT5 requirement, which up-regulates expression of Runx3 and induces expression of a series of pro-survival molecules, including Bcl-2 and Mcl-1 [37, 38]. However, IL7 also activates other downstream signalling pathways, such as PI-3K and NFATc1, which contribute to cell survival by up-regulation of anti-apoptotic molecules and trophic factors, including expression of the glucose transporter-1 [39, 40, 41].
Upon their generation in the thymus, T cells move out to peripheral tissues but they remain addicted to IL7 throughout their life. Thus, maintaining high levels of IL7Rα expression on mature T cells is critical for T cell survival. However, the regulatory mechanism of IL7Rα transcription is quite distinct between thymocytes and peripheral T cells. Previously, an evolutionary conserved enhancer element, CNS1, had been identified that sits 3.6 kb upstream of the IL7Rα promoter [42], and which was found to be controlled by multiple factors, including FoxO1 and Foxp1, as well as glucocorticoids [42, 43, 44]. Remarkably, deletion of CNS1 resulted in dramatic loss of IL7Rα expression and significantly reduced T cell numbers in the periphery, but did not affect IL7Rα expression on thymocytes or decreased thymic cellularity [45]. These results suggested the use of distinct molecular mechanisms to control IL7Rα chain expression on immature and mature T cells, and also echo previous observations of different IL7Rα regulatory mechanisms between $CD4^+$ and $CD8^+$ T cells [12, 31] and also B and T lineage cells [46, 47]. Thus, IL7Rα expression is regulated in a highly specific manner, depending on the developmental stage and possibly also on the activation status of T cells.

3 Regulation of IL7 receptor expression

A distinguishing feature of IL7Rα from other cytokine receptors of the γ_c family is the down-regulation of its own expression by cognate cytokine signalling [12]. In fact, not only IL7, but other γ_c cytokines also transcriptionally suppress IL7Rα [47, 12]. IL7-induced down-regulation of IL7Rα expression is further accelerated by rapid endocytosis and degradation of IL7-associated IL7Rα proteins, so that IL7 induces a negative regulatory feedback loop for IL7 receptor signalling [48, 49]. Considering the critical role of IL7 in T cell survival and the limited availability of IL7 in vivo, it seems paradoxical that IL7 signalling would terminate further IL7 signalling.
Two distinct but not mutually exclusive hypotheses have been put forward to explain the self-limiting nature of IL7 receptor signalling on T cells. The first model proposes that T cells constrain IL7 signalling and consumption to maximise the use of limited extra-cellular IL7 and to maintain clonal diversity of the mature peripheral T cell pool [12]. By preventing excess consumption of IL7 and clonal outgrowth of T cells that have better access to IL7, on a population basis, IL7-induced IL7Rα down-regulation would maximise the size of the T cell pool, while maintaining a high degree of TCR clonal diversity. Thus, IL7Rα down-regulation would be beneficial for a population, but not for individual T cells per se. Contrary to this idea, the second model proposes that sustained IL7 signalling would be detrimental for individual T cells, and that termination of prolonged IL7 signalling is necessary for survival. In fact, in vivo transfer experiments and in vitro proliferation assays with IL7Rα transgenic T cells demonstrated that the inability to down-regulate IL7Rα expression resulted in cytokine-induced cell death of T cells [15]. Specifically, continuous IL7R signalling in $CD8^+$ T cells resulted in their uncontrolled proliferation and rapid differentiation

into effector cytolytic T cells that produced large amounts of interferons and induced cell death. In agreement, IL7Rα-transgenic mice also contain a significantly reduced size of T cell pool in the periphery [12, 15].
The molecular mechanisms that lead to suppression of IL7Rα expression have been assessed, and at least for $CD8^+$ T cells, it was found to be dependent on the zinc finger transcription factor Gfi1 [12]. $CD8^+$ T cells in Gfi1-deficient mice expressed high levels of IL7Rα, while $CD8^+$ T cells in Gfi1-transgenic mice showed reduced IL7Rα transcription and expression [38, 31]. The cellular factors that control IL7Rα suppression in $CD4^+$ T cells are less well known. But reportedly, the forkhead box family transcription factor Foxp3 down-regulates IL7Rα expression on $Foxp3^+$ T regulatory $CD4^+$ T cells [50], and Foxp1 can suppress IL7Rα by antagonising Foxo1 [44]. The precise transcriptional pathway that controls IL7Rα downstream of IL7 and other cytokine signals remains to be mapped.

4 IL7 receptor signalling

Both IL7Rα and γ_c chains lack intrinsic kinase activities. Rather, they require activation of the tyrosine kinases JAK1 and JAK3, which are constitutively associated with the cytosolic tails of IL7Rα and γ_c, respectively, to transduce IL7 signalling [10]. Upon ligand-induced IL7Rα/γ_c hetero-dimerisation, JAK1 and JAK3 trans-activate each other, and subsequently phosphorylate the intracellular tail of IL7Rα. There are three conserved tyrosine residues in the IL7Rα cytosolic domain, but tyrosine 449 is the major substrate of IL7Rα phosphorylation [51]. Phosphorylation of IL7Rα Tyr449 leads to the creation of STAT5 and PI-3-kinase binding sites, resulting in the recruitment and subsequent phosphorylation and activation of these factors [52, 51].
Due to their distinct ligand binding affinities and association with different JAK molecules, the individual contribution of each IL7R subunit to IL7 signalling also differs. The γ_c chain contributes to IL7 receptor signalling through two major activities. Firstly, it serves to bring JAK3 into the receptor signalling complex, which trans-activates IL7Rα-bound JAK1 [10]. Secondly, γ_c dramatically increases the affinity of the IL7 receptor complex for IL7. In the absence of γ_c, IL7Rα binds IL7 with a low affinity [53] ($K_d = 2.4 \times 10^{-10}$ M). However, inclusion of γ_c significantly increases the affinity for IL7 ($K_d = 4 \times 10^{-11}$ M), which results in the preferential capture of IL7 by signalling-competent IL7 receptors compared to signalling-incompetent γ_c-free IL7Rα chain proteins. Whether the high affinity IL7Rα/γ_c complex is only formed upon ligand binding, or whether such high affinity IL7 receptor could be already assembled and expressed on the cell surface is currently a much-debated issue in cytokine biology.
The conventional view posits that the IL7Rα/γ_c complex is formed by stepwise assembly that is triggered by IL7 binding to the IL7Rα chain [54]. In this model, the IL7Rα and γ_c proteins are diffusely distributed in the plasma membrane prior to ligand engagement. Upon IL7 stimulation, IL7Rα binds IL7 with low affinity and undergoes a conformational change that attracts the γ_c chain, which in turn stabilises IL7 binding, to initiate IL7R signalling. The formation of a hetero-trimeric complex of IL7/IL7Rα/γ_c brings the intra-cellular tails of IL7Rα and γ_c into proximity, which juxtapositions and activates JAK1 and JAK3 to initiate downstream signalling.
In an alternative view, it has been proposed that IL7Rα and γ_c can bind even in the absence of IL7, so that γ_c proteins are already sequestered and associated with IL7Rα [16, 55]. In fact, crystallographic studies of the IL7Rα/γ_c receptor complex postulated that IL7Rα and γ_c proteins exist as pre-formed, inactive receptor complexes prior to ligand engagement [16]. In this model, ligand-free IL7Rα and γ_c associate in a "head-to-head" configuration that pushes away the trans-membrane domains and intra-cellular tails of IL7Rα and γ_c, and thus, prevents spontaneous ligand-independent activation of JAK1 and JAK3. Upon IL7 binding, however, the pre-associated IL7Rα/γ_c complex undergoes a conformational change that erects the receptor complex and brings the intra-cellular tails of IL7Rα/γ_c into close proximity and initiates downstream signalling [16].
Currently, it is not clear which one of these strategies is employed by T cells for IL7 receptor signalling. Direct binding of IL7Rα to γ_c proteins on the cell surface could be potentially visualised and quantified by FRET (Fluorescence Resonance Energy Transfer) microscopy. Alternatively, methods such as PLA (Proximity Ligation Assays) could be also employed to demonstrate pre-assembly of γ_c with IL7Rα [56]. At least in human $CD4^+$ T cells, IL7Rα could be co-immunoprecipitated with γ_c in the absence of IL7, which is in support of the IL7Rα/γ_c pre-association model [57]. Whether a stepwise assembly model, where initially all surface IL7 receptors have the same affinity to IL7, or the pre-assembly model, where two classes of IL7 receptor exist and the functionally competent IL7Rα/γ_c complexes would out-compete low affinity IL7Rα receptors, would be more biologically meaningful is not clear. However, we consider this question precisely an area where mathematical modelling can be employed in the near future to compare and test these different hypotheses (or mechanisms) together with empirical data. Thus, in the following section, we illustrate the power of a quantitative mathematical approach by modelling the molecular regulation of IL7R signalling under the scenario where two homeostatic γ_c family cytokines, namely IL7 and IL15, compete for the γ_c chain (see Section 5.1). At the single cell level, we quantify the effect of the altruistic hypothesis on the number of

IL7R molecules expressed on the membrane of T cells (see Section 5.2). Finally, at the population scale, we model the heterogeneity of T cell responses to IL7 stimulation observed in Ref. [58], where IL7 availability and the existence of survival and proliferation thresholds can influence the population dynamics of IL7 dependent T cells (see Section 5.3).

5 Mathematical models at the molecular, cellular and population levels

5.1 Mathematical model at the molecular level

At the molecular level, we are interested in understanding the role of shared components in immune signalling [22]. In the case of IL7R signalling, a first shared component is the γ_c chain, which is part of the hetero-dimeric receptors IL7R and IL15R (see Fig. 1). The γ_c chain is also part of the hetero-trimeric receptor IL2R [59]. In this review, we have chosen to consider the IL15R as a shared component of the IL7 signalling pathway, since there already exists a significant mathematical effort to describe the IL2R one [60, 23, 61, 62, 25].
Let us now describe the shared elements of IL7R and IL15R. In principle, the γ_c receptor subunit can bind to either the IL7Rα or IL15Rβ chains, forming two different hetero-dimeric receptors for IL7 and IL15, respectively.

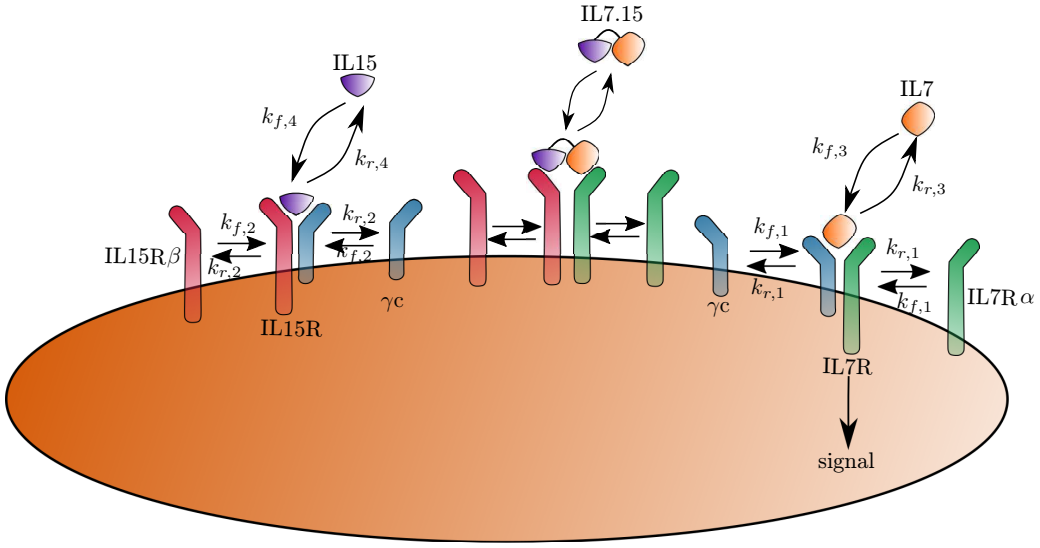

Figure 1: An example of shared molecular components in immune signalling: competition for the γ_c chain by the IL7Rα and IL15Rβ chains (adapted from Ref. [22]).

Although γ_c contributes with the same stoichiometry to each hetero-dimeric receptor (IL7R and IL15R), only when the trimeric complex IL7/IL7Rα/γ_c is internalised, downstream signalling is initiated, as discussed in Section 4 (in Section 5.2 we discuss receptor internalisation in greater detail from a mathematical modelling perspective). Thus, the presence of IL15 can, indirectly, sequester γ_c and, reduce IL7R signalling. Note that we denote by IL7R, the hetero-dimeric receptor composed of one molecular unit of γ_c and one molecular unit of IL7Rα, and by IL15R, the hetero-dimeric receptor composed of one molecular unit of γ_c and one molecular unit of IL15Rβ. In this context, it is important to refer to the recent work by the groups of K. C. García and I. Moraga, who have been able to engineer *synthekines*, namely, engineered ligands, that produce "unnatural" receptor pairings, yet activate distinct signalling programmes [63]. In Fig. 1 we show one such potential synthekine, formed by IL7 and IL15, and denoted IL7.15. In this paper, we do not consider ligand-induced receptor dimerisation (for simplicity, and assume both receptor chains have already formed the hetero-dimeric receptor before ligand binding), although, it may be relevant for some combinations of γ_c and cytokine receptors [18].

5.1.1 Mathematical model

Following Ref. [22], we model the dynamics of free IL7 and IL15 cytokines (or ligands), the receptor subunits γ_c, IL7Rα and IL15Rβ and the (complex) hetero-dimeric receptors IL7R and IL15R, either bound or unbound to their respective ligands. We note that in this review, we do not consider the presence of synthetic ligand IL7.15. We consider the molecular reactions described in Fig. 1, which include the association and dissociation of different receptor chains, as well as the association and dissociation of ligand (IL7 or IL15) to the hetero-dimeric receptors IL7R and IL15R, respectively. We are interested in understanding how the concentrations of these molecular species evolve in time. This is described in Ref. [22] by the following system of ordinary differential equations (ODEs)

$$
\begin{aligned}
\frac{d[\text{IL7R}\alpha]}{dt} &= -k_{f,1}[\text{IL7R}\alpha][\gamma_c] + k_{r,1}[\text{IL7R}]_u \ , \\
\frac{d[\text{IL15R}\beta]}{dt} &= -k_{f,2}[\text{IL15R}\beta][\gamma_c] + k_{r,2}[\text{IL15R}]_u \ , \\
\frac{d[\gamma_c]}{dt} &= -k_{f,1}[\text{IL7R}\alpha][\gamma_c] + k_{r,1}[\text{IL7R}]_u - k_{f,2}[\text{IL15R}\beta][\gamma_c] + k_{r,2}[\text{IL15R}]_u \ , \\
\frac{d[\text{IL7R}]_u}{dt} &= k_{f,1}[\text{IL7R}\alpha][\gamma_c] - k_{r,1}[\text{IL7R}]_u - k_{f,3}[\text{IL7}][\text{IL7R}]_u + k_{r,3}[\text{IL7R}]_b \ , \\
\frac{d[\text{IL15R}]_u}{dt} &= k_{f,2}[\text{IL15R}\beta][\gamma_c] - k_{r,2}[\text{IL15R}]_u - k_{f,4}[\text{IL15}][\text{IL15R}]_u + k_{r,4}[\text{IL15R}]_b \ , \\
\frac{d[\text{IL7R}]_b}{dt} &= k_{f,3}[\text{IL7}][\text{IL7R}]_u - k_{r,3}[\text{IL7R}]_b \ , \\
\frac{d[\text{IL15R}]_b}{dt} &= k_{f,4}[\text{IL15}][\text{IL15R}]_u - k_{r,4}[\text{IL15R}]_b \ . \\
\frac{d[\text{IL7}]}{dt} &= -k_{f,3}[\text{IL7}][\text{IL7R}]_u + k_{r,3}[\text{IL7R}]_b \ , \\
\frac{d[\text{IL15}]}{dt} &= -k_{f,4}[\text{IL15}][\text{IL15R}]_u + k_{r,4}[\text{IL15R}]_b \ .
\end{aligned}
$$

These equations can be solved for different initial conditions of ligand concentration of IL7 and IL15, as well as different number of receptor chains (γ_c, IL7Rα and IL15Rβ) [22] (see Table 1). The table below provides the values of the association and dissociation rates considered in the model [22], and the different initial conditions that have been considered.

parameter	value	units
ρ (cell density)	10^5	cells/μL
[IL7]$(t=0)$	$10^{-1} - 10^3$	nM
[IL15]$(t=0)$	$10^{-1} - 10^3$	nM
[IL7Rα]$(t=0)$	10^3	cell^{-1}
[IL15Rβ]$(t=0)$	10^3	cell^{-1}
[γ_c]$(t=0)$	$10 - 10^5$	cell^{-1}
$k_{f,1}$	1	nM^{-1}min^{-1}
$k_{r,1}$	0.1	min^{-1}
$k_{f,2}$	1	nM^{-1}min^{-1}
$k_{r,2}$	0.1	min^{-1}
$k_{f,3}$	1	nM^{-1}min^{-1}
$k_{r,3}$	0.1	min^{-1}
$k_{f,4}$	0.1	nM^{-1}min^{-1}
$k_{r,4}$	0.1	min^{-1}

Table 1: Summary of parameters used in the molecular model of Section 5.1. Parameter values have been taken from Ref. [58].

In Fig. 2 (left plot) we show the effect of the initial concentration of IL7, [IL7]$(t=0)$, on the steady state value of

the relative fraction of bound IL7 receptors, $[\text{IL7R}]_b$, defined as follows:

$$f_7 = \lim_{t \to +\infty} \frac{[\text{IL7R}]_b(t)}{[\text{IL7R}]_b(t) + [\text{IL15R}]_b(t)} \,. \tag{1}$$

Fig. 2 (middle plot) shows the effect of the initial concentration of IL15, $[\text{IL15}](t = 0)$, on f_7. We note that f_7 decreases as the initial concentration of $[\text{IL15}](t = 0)$ increases, as expected. The green curve in Fig. 2 can be reproduced using the language BioNetGen [64, 65, 66] and the listing in Appendix A. Minimal modifications of the code will allow the reader to obtain the rest of the plots in Fig. 2. Finally, the right plot, shows for an initial concentration of $[\text{IL15}] = 9.5\text{nM}$ (the IL15 concentration that yields $[\text{IL7R}]_b = [\text{IL15R}]_b$ at steady state), the effect of the initial value of γ_c chain expression on the steady state values of $[\text{IL7R}]_b$ and $[\text{IL15R}]_b$.

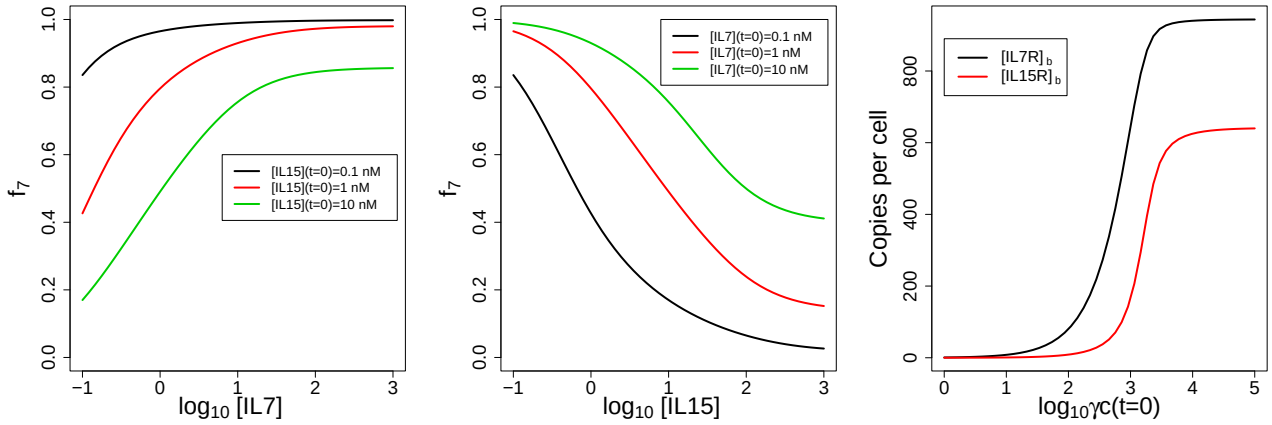

Figure 2: Left plot: fraction of bound $[\text{IL7R}]_b$, f_7, as defined by Eq. (1), for different values of the initial concentration of $[\text{IL7}](t = 0)$. Different colours correspond to different values of the initial concentration of $[\text{IL15}](t = 0)$, as shown in the legend. Middle plot: fraction of bound $[\text{IL7R}]_b$, f_7, as in the left panel, but as a function of the initial concentration of $[\text{IL15}](t = 0)$. Right plot: steady state values for the bound complexes, $[\text{IL7R}]_b$ and $[\text{IL15R}]_b$, as a function of the initial γ_c chain expression, $\gamma_c(t = 0)$. The parameters have been taken from Ref. [58] and have been summarised in Table 1.

5.2 Mathematical model at the cellular level

The role of the IL7 receptor in T cell development, homeostasis and differentiation has been widely studied and recognised [19, 67]. IL7Rα cell surface expression on T cells is down-regulated once a T cell has received enough survival signals mediated by IL7R [19, 12]. To model this so-called *altruistic* down-regulation of membrane IL7R, we note that, upon IL7 stimulation, there is rapid IL7Rα internalisation (mediated by endocytosis), that is accompanied with a reduced rate of receptor recycling and increased receptor degradation [48]. Thus, we first formulate a simple mathematical model (for further details, see Ref. [24]), which describes the dynamics of the number of *ligand molecules* (IL7, in this case), $m_1(t)$, and per cell free-receptor (IL7R), $m_2(t)$, binding/unbinding to form a receptor-ligand bound complex, $m_3(t)$, internalisation, degradation and recycling. We also assume that cell signalling is elicited (and encoded in the dynamics of the variable, $m_4(t)$, which represents a potential unidentified transcription factor), after bound receptors are internalised, as reported in Ref. [48]. Finally, the altruistic effect [12] is included as a signal-dependent synthesis rate [24]. We note that recent experimental evidence suggests that IL7 availability is regulated by innate lymphoid cells (ILCs), which act as a "cytokine sink" by competing for and consuming IL7 and thus, restricting T cell homeostasis in lymphoid organs. In fact, ILCs seem to outcompete T cells for IL7 by resisting IL7-mediated IL7R down-regulation [68], which would support the idea that ILCs do not behave in an altruistic manner.

5.2.1 A simple model of altruistic IL7Rα dynamics

Mathematically, we describe the time evolution of the IL7 and IL7R in a cellular model (see Ref. [24]) making use of a system of ordinary differential equations (ODEs), as follows

$$\frac{dm_1}{dt} = \phi + N_c(k_{\text{off}}\, m_3 - k_{\text{on}}\, m_1\, m_2)\ , \tag{2}$$

$$\frac{dm_2}{dt} = -k_{\text{on}}\, m_1\, m_2 + k_{\text{off}}\, m_3 - \sigma_u\, m_2 + \frac{\kappa_s}{\kappa_s + m_4}\xi\ , \tag{3}$$

$$\frac{dm_3}{dt} = k_{\text{on}}\, m_1\, m_2 - k_{\text{off}}\, m_3 - \sigma_b\, m_3\ , \tag{4}$$

$$\frac{dm_4}{dt} = \psi\, m_3 - \chi\, m_4\ , \tag{5}$$

where

- ϕ is the rate at which free IL7 is replenished in the extra-cellular volume (source term),
- N_c is the total number of cells (in the experiment),
- k_{on} and k_{off} are, respectively, the binding and unbinding rates of IL7 and IL7R,
- σ_u and σ_b are the internalisation rates of the unbound and bound receptors (following Ref. [48] and Ref. [24], we assume $\sigma_b > \sigma_u$),
- ξ is the rate at which IL7R receptor is synthesised and transported to the cell membrane,
- κ_s is the carrying capacity of m_4, which accounts for the altruistic effect. Note that in the limit $\kappa_s \to 0^+$ we have perfect altruism (as IL7R synthesis after receptor internalisation is fully inhibited). On the other hand, in the limit $\kappa_s \to +\infty$, the rate of synthesis is independent of signalling, and thus, there is no altruistic feedback (as might be the case for ILCs [68]) [1],
- ψ is the rate at which internalised bound receptors elicit a signal (encoded by the potential unidentified transcription factor, m_4), and
- χ is the characteristic degradation rate of the signal (encoded by the potential unidentified transcription factor, m_4).

5.2.2 Steady state analysis of the cellular model

In steady state, the system of equations, Eq. (2) to Eq. (5), can be solved analytically. The solution is given by

$$m_1^{ss} = \frac{\phi(k_{\text{off}} + \sigma_b)\sigma_u(\kappa_s N_c \sigma_b \chi + \phi\psi)}{k_{\text{on}}\sigma_b\left[\kappa_s N_c \sigma_b \chi(N_c\xi - \phi) - \phi^2\psi\right]}\ , \tag{6}$$

$$m_2^{ss} = \frac{1}{N_c\sigma_u}\left[\frac{\kappa_s N_c^2 \sigma_b \xi \chi}{\kappa_s N_c \sigma_b \chi + \phi\psi} - \phi\right]\ , \tag{7}$$

$$m_3^{ss} = \frac{\phi}{N_c\sigma_b}\ , \tag{8}$$

$$m_4^{ss} = \frac{\phi\psi}{N_c\sigma_b\chi}\ . \tag{9}$$

These steady state solutions are positive as long as

$$\phi < \phi_{\text{threshold}} \equiv \frac{\sqrt{\kappa_s N_c^2 \sigma_b \chi(\kappa_s \sigma_b \chi + 4\psi\xi)} - \kappa_s N_c \sigma_b \chi}{2\psi}\ .$$

Note that the limit, $\kappa_s \to +\infty$, in the steady state solutions given above, corresponds to a receptor-ligand system in which no cellular altruistic behaviour is present. Let us now assess the effect of altruism in the different observables

[1] If the intra-cellular levels of the potential transcription factor, m_4, are such that $m_4 \gg \kappa_s$, the synthesis rate is considerably reduced.

Parameter	Value	Units
ϕ	$10^1 - 10^8$	receptor hour^{-1}
ξ	1.2×10^3	receptor hour^{-1}
κ_s	10^3	signal
σ_U	0.14	hour^{-1}
σ_B	1.4	hour^{-1}
$k_{\text{off}}/k_{\text{on}}$	1.7	ng ml^{-1}
ψ	0.61	signal receptor^{-1} hour^{-1}
χ	0.19	hour^{-1}

Table 2: Parameters of the cellular model taken from Ref. [24] and Ref. [48].

of the cellular system. For instance, in Fig. 3 we plot $\frac{m_1^{ss}(\kappa_s \to +\infty)}{m_1^{ss}(\kappa_s)}$, the steady state ratio of free (available for other cells) IL7 in the non-altruistic ($\kappa_s \to +\infty$) and altruistic ($\kappa_s \neq 0$) cases, for different values of ϕ (left plot) and for different values of κ_s (right plot). Similarly, in Fig. 4 we plot $\frac{m_2^{ss}(\kappa_s)}{m_2^{ss}(\kappa_s \to +\infty)}$, the steady state ratio of free receptors (IL7R) in the non-altruistic ($\kappa_s \to +\infty$) and altruistic ($\kappa_s \neq 0$) cases, for different values of ϕ (left plot) and for different values of κ_s (right plot). Note the symmetry between Fig. 3 and Fig. 4. This is due to the fact that in steady state, one can show

$$\lim_{t \to +\infty} [\text{IL7}](t)[\text{IL7R}]_u(t) = \frac{\phi(k_{\text{off}} + \sigma_b)}{k_{\text{on}} N_c \sigma_b} , \tag{10}$$

which does not depend on the value of κ_s, the parameter which encodes the level of altruism in the IL7 signalling system.

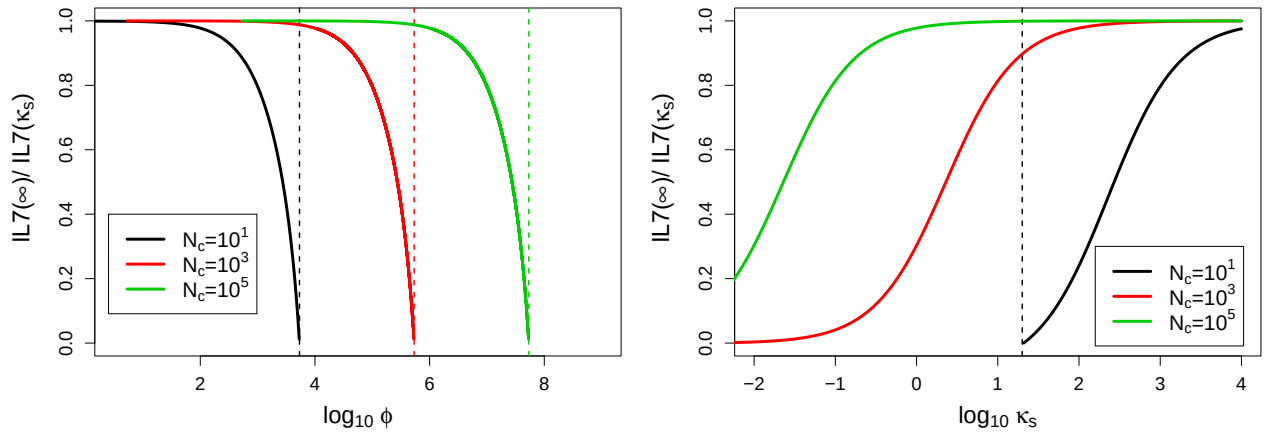

Figure 3: Effect of signalling altruism on the amount of available extra-cellular (free) IL7. Left plot: effect of ϕ for $\kappa_s = 10^3$ on $\frac{m_1^{ss}(\kappa_s \to +\infty)}{m_1^{ss}(\kappa_s)}$ for different values of N_c. Right plot: effect of κ_s for $\phi = \phi_{\text{threshold}}/2$ on $\frac{m_1^{ss}(\kappa_s \to +\infty)}{m_1^{ss}(\kappa_s)}$ for different values of N_c. Model parameters are summarised in Table 2. Different colours correspond to different values of the number of cells, N_c, in the experiment.

5.3 Mathematical model at the population level

Naive CD8$^+$ T cells require signalling-mediated by the cytokine interleukin-7 (IL7) for survival and proliferation [67]. As discussed in Palmer *et al.* [58], CD8$^+$ T cells have distinct thresholds for survival and proliferation; that is, a stronger IL7R-mediated signal is required for proliferation as compared to the strength of signal required for cellular survival. Recent experiments also support the idea that higher CD5 expression correlates with higher IL7R expression in CD8$^+$ T cells, and indeed CD5$^{\text{hi}}$ T cells were found to have more robust responses to IL7 than CD5$^{\text{lo}}$

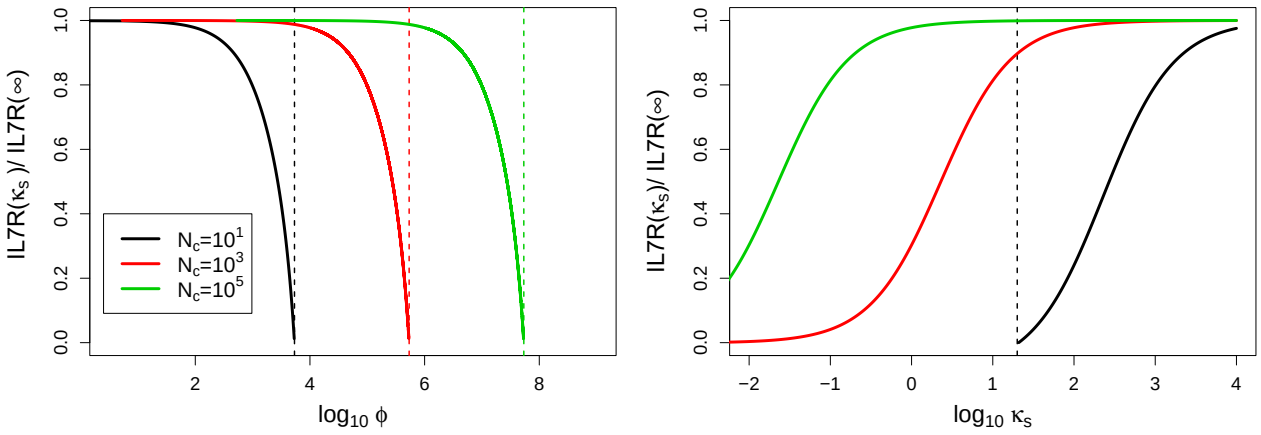

Figure 4: Effect of altruism on the amount of free IL7R. Left plot: effect of ϕ for $\kappa_s = 10^3$ on $\frac{m_2^{ss}(\kappa_s)}{m_2^{ss}(\kappa_s \to +\infty)}$ for different values of N_c. Right plot: effect of κ_s for $\phi = \phi_{\text{threshold}}/2$ on $\frac{m_2^{ss}(\kappa_s)}{m_2^{ss}(\kappa_s \to +\infty)}$ for different values of N_c. Model parameters are summarised in Table 2. Different colours correspond to different values of the number of cells, N_c, in the experiment.

T cells [58]. On the other hand $CD5^{lo}$ T cells were found to have prolonged survival when compared to $CD5^{hi}$ T cells in an IL7 independent environment [58].

In this section, we develop a mathematical model at the population level of immune IL7R-mediated signalling that considers the heterogeneity of the expression levels observed for CD5 and IL7R. We introduce, thus, four different $CD8^+$ T cell populations (see Fig. 5), characterised by their relative expression of these two proteins. We also assume the total pool of $CD8^+$ T cells exists within a well-mixed system, such that there exists a global concentration of IL7. Thus, we neglect any spatial heterogeneities. T cells may receive signals for survival or proliferation depending on the amount of available extra-cellular IL7 and their relative IL7R surface expression. Since we are considering the dynamics of T cells at the population scale, we assume the effects of localised IL7 production and consumption at the single cell scale, are effectively "averaged out" allowing the modelling effort to give a reasonable description of the population dynamics [22, 24].

The physical size of the IL7 protein is much smaller than the size of a T cell and typically there are many more of these molecules than T cells in the experimental system. Our measurement of IL7 will therefore not be based on the number of IL7 molecules, but rather the concentration of IL7 in the extra-cellular medium. Therefore, we use a deterministic characterisation for the IL7 concentration, instead of a stochastic description, which shall be introduced to describe the number of T cells in the system. We assume the rate of production of IL7 is independent of the number of T cells [69], and for the purposes of this model, we will assume the rate of IL7 production to be constant. We also assume the rate of consumption of IL7 is proportional to the product of the concentration of IL7 and the number of T cells expressing IL7R, due to the internalisation of ligand-receptor bound complexes (see Section 5.1). The constants of proportionality are greater/lower for $IL7R^{hi}$/$IL7R^{lo}$ T cells, respectively. We further assume that the four different T cell populations have a basal IL7-independent death rate. This death rate is greater for $CD5^{hi}$ T cells than for $CD5^{lo}$ T cells [58]. However this death rate does not depend on the level of IL7R expression (see Fig. 5). The death rate is switched on if IL7 availability is below a given survival threshold and equivalently, it is switched off if the concentration of IL7 is above this threshold [58]. Similarly, if the concentration of IL7 is above a given proliferation threshold, we turn on a proliferation term for $IL7R^{hi}$ T cells. Following a division event $IL7R^{hi}$ T cells produce two daughter cells, in the corresponding $IL7R^{lo}$ pool, in consonance with the altruistic hypothesis. We assume $IL7R^{lo}$ T cells may not receive sufficient IL7 stimulus to undergo a division event. $IL7R^{lo}$ T cells are assumed to up-regulate their expression levels of IL7R and become $IL7R^{hi}$ (see Fig. 5). Lastly, we assume the level of CD5 expression is invariant; that is, $CD5^{hi}$ cells can only increase or decrease their levels of IL7R expression, but maintain their high level of CD5 expression constant. The same is true for $CD5^{lo}$ cells (see Fig. 5). The interplay between IL7 receptor expression and signalling on the fate (division, proliferation or IL7R up-regulation) of the four different population of $CD8^+$ T cells can be captured mathematically and will be discussed in the following section.

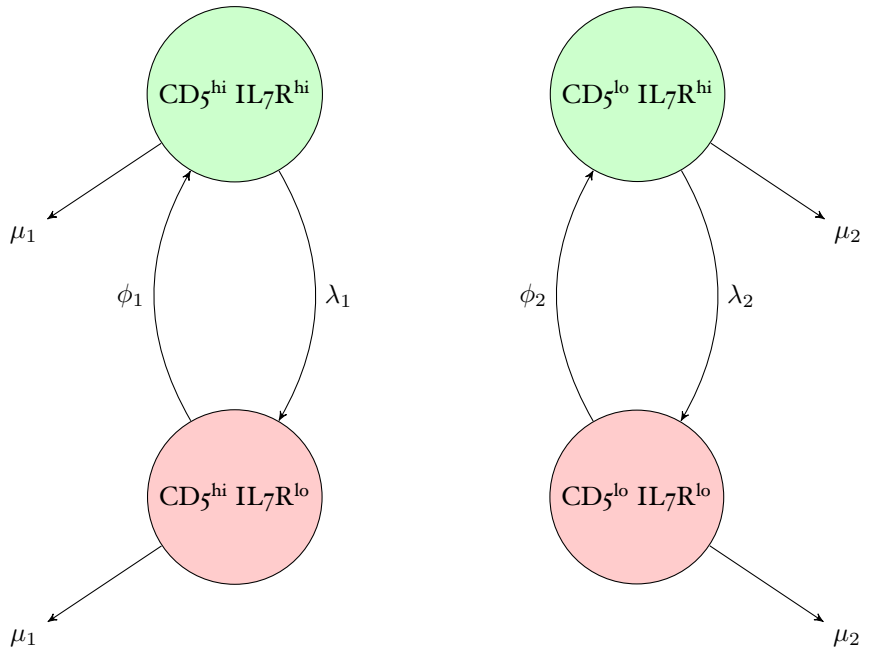

Figure 5: Immune signalling at the population level: possible transitions between the four subsets of the peripheral CD8$^+$ T cell pool. We impose $\mu_1 > \mu_2$; that is, CD5^{lo} T cells have prolonged survival in a cytokine independent environment. In the mathematical model the parameter λ corresponds to the per cell division rate. λ_1 is the per cell division rate for CD5^{hi} CD8$^+$ T cells and λ_2 is the per cell division rate for CD5^{lo} CD8$^+$ T cells, with $\lambda_1 > \lambda_2$ [58]. We assume that after a division event, there is a significant drop in the level of IL7R expressed on the surface of a cell, since daughter cells inherit, on average, half of the IL7 receptors expressed by their mother cell. Finally, ϕ corresponds to the basal up-regulation rate of IL7R expression and is assumed to be independent of the extra-cellular IL7 concentration. ϕ_1 is the per cell IL7R up-regulation rate for CD5^{hi} CD8$^+$ T cells and ϕ_2 is the per cell IL7R up-regulation for CD5^{lo} CD8$^+$ T cells.

5.3.1 Mathematical model

We denote by $n_{i,j}$ the number of cells in subset $S_{i,j}$: an index value of "1" always refers to "high", whereas an index of "2" always refers to "low". If a pair of indexes appears in a variable, the first one refers to CD5 and the second to IL7R, respectively. Specifically, we have defined

cell type	variable
CD5^{hi}IL7R^{hi}	$n_{1,1}$
CD5^{hi}IL7R^{lo}	$n_{1,2}$
CD5^{lo}IL7R^{hi}	$n_{2,1}$
CD5^{lo}IL7R^{lo}	$n_{2,2}$

We now describe the dynamics that characterise the four different population of CD8$^+$ T cells and that are driven by IL7 signalling.

Dynamics of IL7 We model the concentration of IL7 in a deterministic manner, as we argued above. Let I denote the concentration of IL7. We assume IL7 is produced at a constant rate ν, independent of its extra-cellular level [9, 7]. We also consider IL7 loss, due to internalisation of IL7 once it binds IL7R expressed on the surface of T cells. We, thus, assume that this loss term is proportional to the global concentration of IL7 and the number of T cells. These terms then take the form

$$-\gamma_1(n_{1,1} + n_{2,1})I - \gamma_2(n_{1,2} + n_{2,2})I \ ,$$

where $\gamma_1 > \gamma_2$, since we assume IL7R$^{\text{hi}}$ cells internalise IL7 at a faster rate than IL7R$^{\text{lo}}$ cells, since their IL7R surface expression levels are higher by construction. The concentration of IL7 then obeys an ODE of the form

$$\frac{dI}{dt} = \nu - \gamma_1(n_{1,1} + n_{2,1})I - \gamma_2(n_{1,2} + n_{2,2})I \ . \tag{11}$$

Dynamics of T cells The populations of CD8$^+$ T cells are modelled in a stochastic fashion. Let us introduce a threshold for survival θ_s and a threshold for proliferation θ_p [58, 24]. We shall assume the dimensions of θ_s and θ_p to be those of I, *i.e.,* volume concentration. We assume that the survival threshold is lower than the proliferation one [24]; that is, $\theta_s < \theta_p$. We now describe the CD8$^+$ T cell dynamics, as follows:

- If $I < \theta_s$ (death event):
  $n_{i,j} \to n_{i,j} - 1$, in a small time interval, Δt, with probability $\mu_i \ n_{i,j} \ \Delta t$ for $i, j = 1, 2$.
- If $\theta_s < I < \theta_p$ (survival event):
  $n_{i,j} \to n_{i,j}$, in a small time interval, Δt, with probability one for $i, j = 1, 2$.
- If $\theta_p < I$ (proliferation event):
  $\left.\begin{array}{l} n_{i,1} \to n_{i,1} - 1 \\ n_{i,2} \to n_{i,2} + 2 \end{array}\right\}$ in a small time interval, Δt, with probability $\lambda_i \ n_{i,1} \ \Delta t$ for $i = 1, 2$.
- Finally, and given that the up-regulation of IL7R is independent of the concentration of IL7, this transition takes the form:
  $\left.\begin{array}{l} n_{i,2} \to n_{i,2} - 1 \\ n_{i,1} \to n_{i,1} + 1 \end{array}\right\}$ in a small time interval, Δt, with probability $\phi_i \ n_{i,2} \ \Delta t$ for $i = 1, 2$.

These transitions are illustrated in Figure 5.

Threshold function We assume the probabilities of death and proliferation events to be non-zero only when the concentration of IL7 is below or above the respective threshold functions for survival and proliferation. The existence of these survival and proliferation thresholds have been experimentally observed [58]. We, therefore, choose a function such that when the concentration is above or below a certain threshold, it is either 0 or 1. One such suitable function is the logistic function, defined as follows:

$$f_s(I) = \frac{1}{1 + e^{\alpha(I - \theta_s)}} \qquad \text{and} \qquad f_p(I) = \frac{1}{1 + e^{\alpha(\theta_p - I)}} \ . \tag{12}$$

We choose the dimensions of α to be inverse concentration, such that the value of $f_s(I)$ is a dimensionless quantity bounded between 0 and 1. This threshold function is then included within the previously defined transition probabilities for death and proliferation events. If $f_\bullet(I) \approx 0$, then the probability of the given event is close to zero and the event is effectively turned off. Similarly if $f_\bullet(I) \approx 1$, then the probability of the event is turned on.
The parameter α modulates the *severity* of the threshold function. In particular, if $\alpha \to +\infty$, the threshold is extremely sharp. In fact, we have

$$\lim_{\alpha \to +\infty} f_s(I) = \lim_{\alpha \to +\infty} \frac{1}{1 + e^{\alpha(I - \theta_s)}} = \begin{cases} 0 & \text{if} \quad I > \theta_s \ , \\ 1/2 & \text{if} \quad I = \theta_s \ , \\ 1 & \text{if} \quad I < \theta_s \ . \end{cases}$$

In Fig. 6 we show the threshold functions (see Eq. (12)) for different values of α. In the limit $\alpha \to 0^+$, the thresholds disappear and T cell proliferation and death events do not depend on the amount of free IL7 available. On the other hand, in the limit $\alpha \to +\infty$ the

5.3.2 Numerical results

We have implemented the model discussed in Section 5.3.1, making use of a deterministic characterisation (ODE) for the concentration of IL7, $I(t)$, and either an ODE model for the number of cells in each *compartment* or a stochastic Markov description, which requires the implementation of a Gillespie algorithm (see code provided in Appendix B).

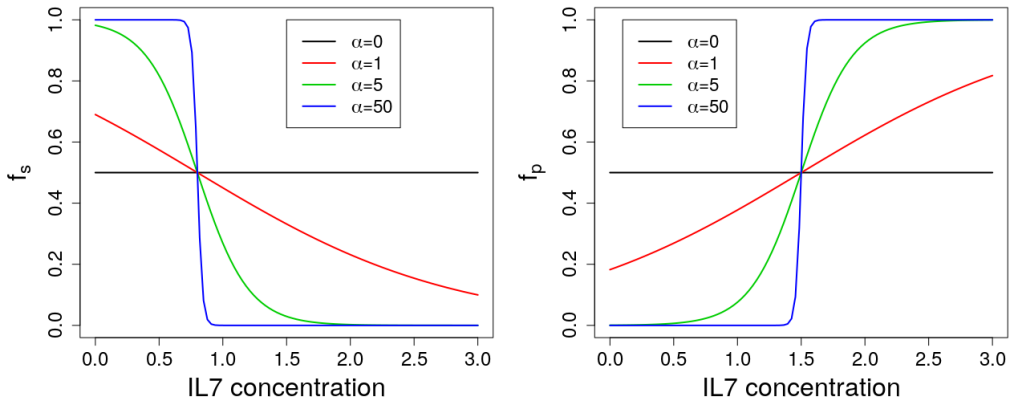

Figure 6: Effect of the parameter α on the severity of the threshold functions (see Eq. (12)). Note that for $\alpha = 0$ (black line) the threshold functions are constant and equal to $\frac{1}{2}$. On the other hand, for $\alpha \gg 1$ the functions are almost discontinuous and the thresholds rather sharp.

The deterministic model for the four T cell populations and the concentration of IL7 is described in the code provided in Appendix C. The parameters used in the numerical studies have been summarised in Table 3. When other parameter values have been used, we have provided their values explicitly. To model different extra-cellular signalling environments, describing different values of extra-cellular IL7 concentration, we vary the value of the parameter ν, and make use of a *soft* threshold given by $\alpha = 5$. As shown in Figs. 7-9, different values of ν change the steady state of the four T cell populations. In all cases, on the right panel we show the relative number of T cells with high (black lines) and low (red lines) expression of CD5. In that panel we also show two different stochastic simulations to emphasise the role of fluctuations when the number of cells is small (in all cases we have considered that, initially, there is a total of 200 cells, equally distributed between the four compartments). For completeness, in Fig. 10 we consider the case where IL7 is removed from the system not only by IL7 receptor-mediated internalisation but by other mechanisms (that we denote generically, *degradation*), for the same parameter values as those of Fig. 9. Note that, while the maximum level of IL7 changes significantly, the dynamics of the $CD8^+$ T cell populations does not qualitatively change.

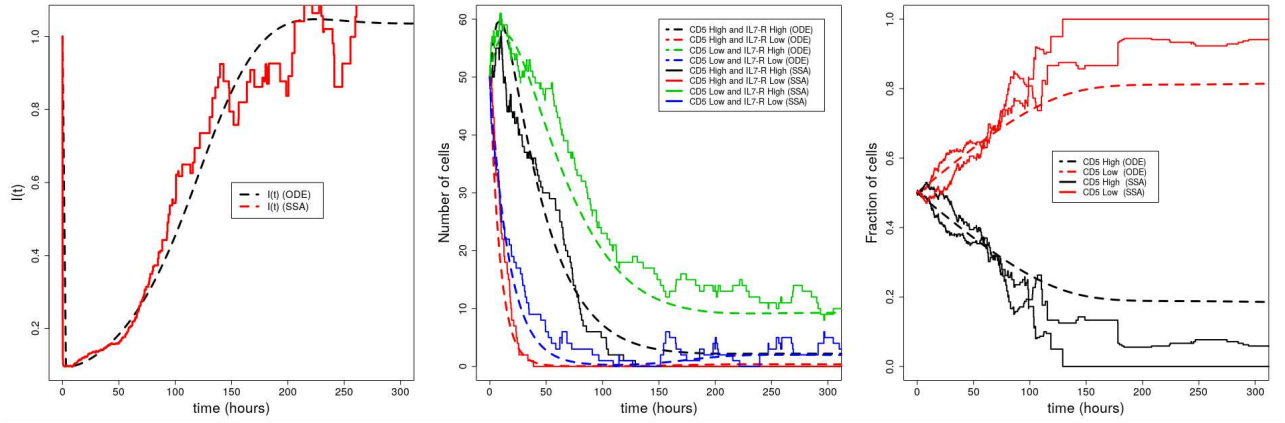

Figure 7: Numerical study for a total time of two weeks with low IL7 production, $\nu = 1$ and a *soft* threshold, $\alpha = 5$. On the right plot, we see the T cell population is dominated by the subset of $CD5^{lo}$ T cells. Note the reasonable agreement between the deterministic model (ODE) and the stochastic simulations (SSA). On the left plot, we follow the extra-cellular IL7 concentration in time. On the middle plot, we follow the four cellular populations in time. On the right plot, we follow the two cellular populations, as defined by their CD5 expression in time.

From these numerical studies, two significant conclusions can be derived. First of all, different values of ν (the

parameter	value	units	reference
$I(0)$	1	[con]	Note 1
$n_{1,1}(0)$	50	cells	This work
$n_{1,2}(0)$	50	cells	This work
$n_{2,1}(0)$	50	cells	This work
$n_{2,2}(0)$	50	cells	This work
ν	50	$[\text{con}]^{-1}\text{hour}^{-1}$	Note 2 [24]
γ_1	0.08	hour^{-1}	[24]
γ_2	0.02	hour^{-1}	Chosen to be $\sim \gamma_1/4$
μ_1	0.027	hour^{-1}	[24]
μ_2	0.018	hour^{-1}	Chosen to be $= 2\mu_1/3$
λ_1	0.083	hour^{-1}	[24]
λ_2	0.055	hour^{-1}	Chosen to be$= 2\lambda_1/3$
ϕ_1	0.083	hour^{-1}	Chosen to be $= \lambda_1$
ϕ_2	0.042	hour^{-1}	Chosen to be $\sim \phi_1/2$
θ_s	0.8	[con]	This work
θ_p	1.5	[con]	This work
α	5	$[\text{con}]^{-1}$	Note 3
δ	20	h^{-1}	[24]

Table 3: Parameters for the population model of IL7-mediated signalling. Note 1: we normalise the initial concentration of IL7 to 1. This allows us to use generic units of concentration ([con]) rather than the standard M (moles/litre). Note 2: we have normalised ν from Ref. [24] according to Note 1. Note 3: in order to guarantee a threshold-like response, we have chosen a relatively large value of α.

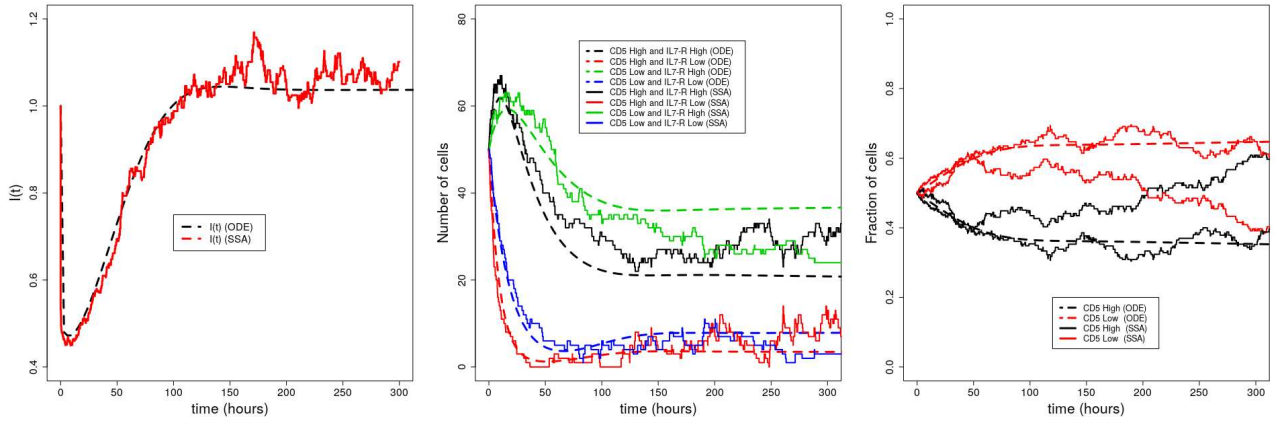

Figure 8: Numerical study for a total time of two weeks with medium IL7 production, $\nu = 5$ and a *soft* threshold, $\alpha = 5$. On the right plot, we see the T cell population is dominated by the subset of $CD5^{lo}$ T cells. Note that a deterministic (ODE) approach cannot precisely reproduce the stochastic behaviour (SSA). On the left plot, we follow the extra-cellular IL7 concentration in time. On the middle plot, we follow the four cellular populations in time. On the right plot, we follow the two cellular populations, as defined by their CD5 expression in time.

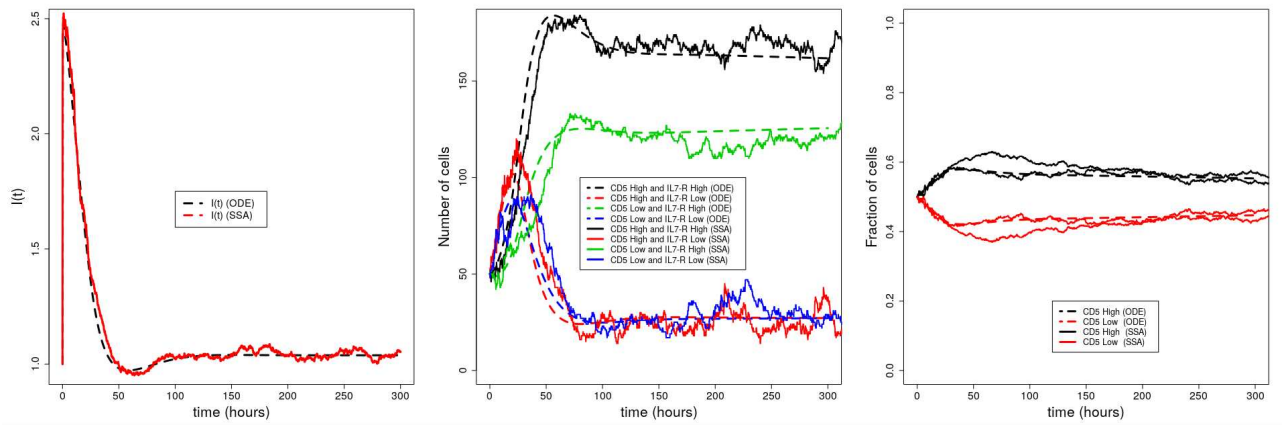

Figure 9: Numerical study for a total time of two weeks with high IL7 production, $\nu = 25$ and a *soft* threshold, $\alpha = 5$. On the right plot, we see the T cell population is dominated by the subset of $CD5^{hi}$ T cells. Note that a deterministic (ODE) approach is able to reproduce the stochastic behaviour (SSA). On the left plot, we follow the extra-cellular IL7 concentration in time. On the middle plot, we follow the four cellular populations in time. On the right plot, we follow the two cellular populations, as defined by their CD5 expression in time.

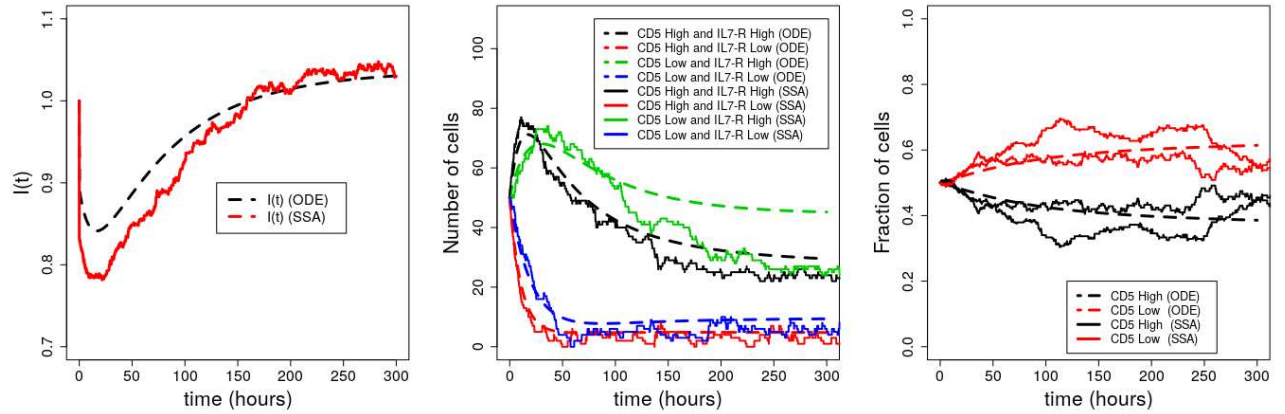

Figure 10: Numerical study for a total time of two weeks with high IL7 production, $\nu = 25$ and a *soft* threshold, $\alpha = 5$. This study also considers the role of IL7 degradation (with rate $\delta = 20\,\mathrm{h}^{-1}$). On the right plot, we see the T cell population is dominated by the subset of $CD5^{lo}$ T cells. Note that a deterministic (ODE) approach cannot precisely reproduce the stochastic behaviour (SSA) observed. On the left plot, we follow the extra-cellular IL7 concentration in time. On the middle plot, we follow the four cellular populations in time. On the right plot, we follow the two cellular populations, as defined by their CD5 expression in time.

parameter that encodes the IL7 extra-cellular environment) lead to different relative fractions of cells with high and low expression of CD5. These results are in agreement with the experimental evidence summarised by Palmer *et al.* [58]. These authors observed population dominance in favour of $CD5^{hi}$ $CD8^{+}$ T cells in high IL7 environments. In contrast, $CD5^{lo}$ $CD8^{+}$ T cells were observed to dominate the T cell repertoire in low IL7 environments. In between these, at physiological levels of IL7, an equal balance in the T cell repertoire was observed [58]. Secondly, the striking result that the deterministic approximation (ODE) cannot capture the *switch* between low and high IL7 extra-cellular environments occurring for intermediate values of ν (see, for instance, the right panel in Fig. 8). This discrepancy between the deterministic and the stochastic descriptions raises a potential methodological concern; namely, how to choose the value of α. We note that these differences originate from two possible effects: the value of ν and that of α. The first effect is easier to understand, since very large values of ν (see, for instance, Fig. 9) drive the cytokine concentration, I, to its deterministic value and stochastic fluctuations are damped out quickly (compare the left plots of Fig. 7 and Fig. 8 to the left plot of Fig. 9). In order to decipher the role of α, we first note that when $\alpha = 0$, the T cell populations do not perceive any IL7 threshold behaviour and their dynamics is independent of the amount of free extra-cellular IL7 available. Secondly, let us now evaluate the effect of different values of α (and the severity of the thresholds) in the dynamics of the four T cell populations. Fig. 11 reproduces the simulations of Fig. 8 for $\alpha = 0$ (top) and $\alpha = 50$ (bottom). As discussed above, the case $\alpha = 0$ is not biologically relevant, since the IL7 survival and proliferation thresholds have been observed in experiments [58]. Furthermore, for the death and proliferation rates obtained in Ref. [24], and in the absence of IL7 survival and proliferation thresholds, the number of T cells increases indefinitely (see middle panel of the top row in Fig. 11). Finally, a comparison between the cases $\alpha = 5$ (see Fig. 8) and $\alpha = 50$ (see bottom row of Fig. 11) shows that sharper threshold functions decrease the size of the stochastic fluctuations.

In order to further dissect our latter claim, in Fig. 12 we show the histogram of stochastic steady states for $\nu = 5$ and for $\alpha = 5$ or $\alpha = 50$. Remarkably, the histogram is so wide that it contains stochastic realisations where there is a switch between the $CD5^{hi}$ and $CD5^{lo}$ populations, that cannot be predicted by the deterministic model. This behaviour suggest that, the combination of non-linearities (in our case the threshold functions) and a stochastic description, leads to richer outcomes than traditional deterministic approaches. It is beyond the scope of this manuscript to study in greater depth the interplay between stochasticity and threshold responses. Yet, we feel this interplay deserves further analysis since it has not been comprehensively addressed in the literature.

6 Dysregulation of IL7 receptor expression and signalling in cancer and inflammation

Direct evidence for the importance of understanding IL7R Biology comes from clinical settings where dysregulation of IL7R expression or signalling were found to be linked with autoimmune inflammatory diseases and tumourigenesis [70, 71]. Both gain- and loss-of-function mutations in the IL7Rα gene have been reported, and there are strong associations between dysregulation of IL7R expression and multiple inflammatory diseases, but also cancer [72, 73]. Along these lines, about 10% of pediatric T-ALL patients displayed gain-of-function mutations in IL7Rα, which caused ligand-independent activation and signalling of IL7R [74, 75, 76]. Most of these mutations were found in exon 6 of the IL7Rα gene, at sites that corresponded to the membrane-proximal region of the extra-cellular domain of the receptor. These mutations could cause homo-dimerisation of IL7Rα molecules as they introduced, among others, new cysteine residues which could form disulfide linkage with other mutated IL7Rα proteins. Remarkably, in these tumour cells, IL7Rα homo-dimerisation was sufficient to induce ligand independent IL7Rα signalling, resulting in constitutive STAT5 phosphorylation and activation [74]. Interestingly, earlier studies indicated that homo-dimerisation of IL7Rα could not trigger IL7R signalling and that signalling required hetero-dimerisation with γ_c receptors, presumably because JAK1 activation required the trans-phosphorylation by JAK3 [11]. Why and how IL7Rα mutations in ALL tumour cells can induce productive signalling by IL7Rα homo-dimerisation is an intense area of research, and insights from structural biology in conjunction with mathematical modelling are expected to shed light on these open and challenging questions.

As a potential explanation, a recent study suggested the role for IL7Rα trans-membrane domains in the spatial reorganisation of mutant IL7Rα homo-dimeric proteins [77]. Under normal circumstances, IL7Rα homodimers would dimerise into a configuration where the intra-cellular domains would all face the same direction and JAK1 molecules would not be juxta-positioned and face each other for trans-phosphorylation. In some IL7Rα mutants, however, twists in the trans-membrane domain would cause rotations of the intra-cellular region which would position JAK1 molecules into the correct orientation for trans-phosphorylation and activation [78].

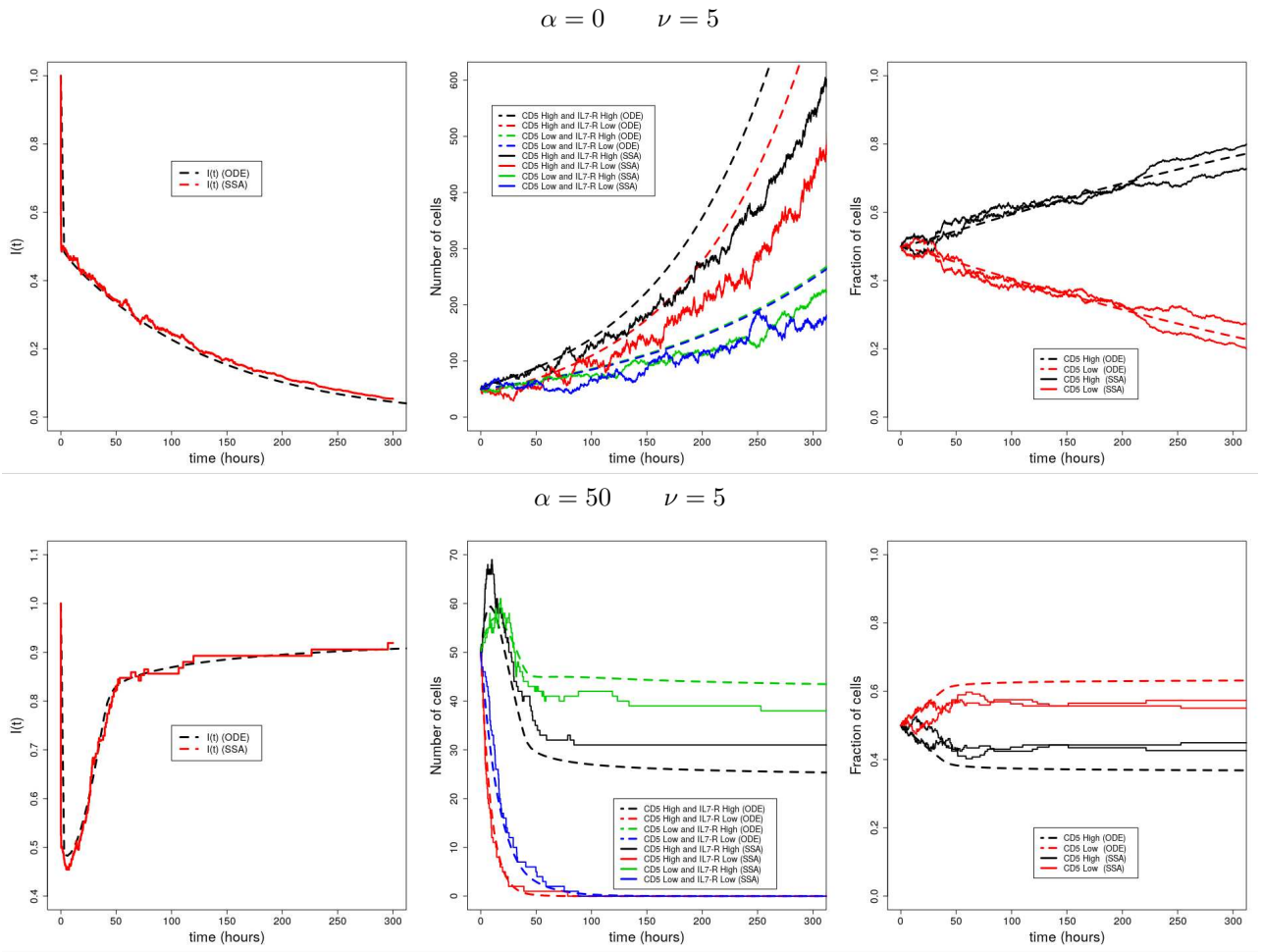

Figure 11: Numerical study for a total time of two weeks with high IL7 production, $\nu = 5$ for two values of α: $\alpha = 0$ (top row) and $\alpha = 50$ (bottom row). On the left plot, we follow the extra-cellular IL7 concentration in time. On the middle plot, we follow the four cellular populations in time. On the right plot, we follow the two cellular populations, as defined by their CD5 expression in time.

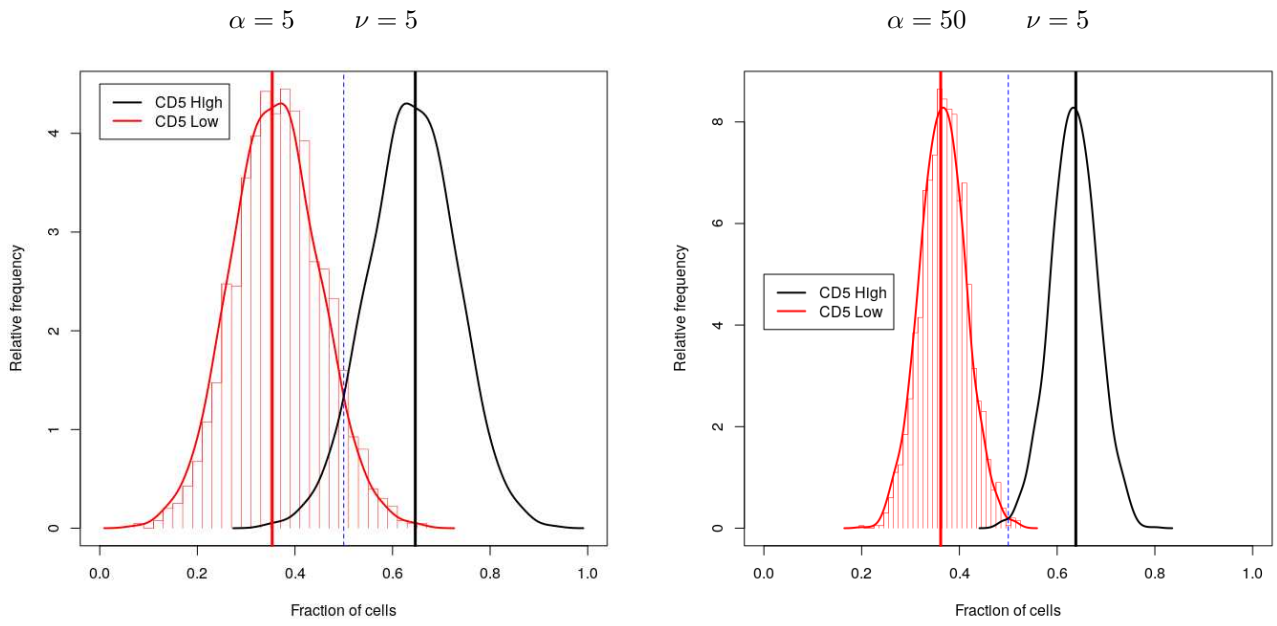

Figure 12: Histogram of the steady state of CD5 high subpopulation (black) and CD5 low subpopulation (red) for $\nu = 5$ and $\alpha = 5$ (left) or $\alpha = 50$ (right). The blue dashed vertical line is a guide to the eye to show the line where the fraction of each subpopulation is 50%.

Beyond the implications in tumour biology, these findings raise many challenging questions, such as why persistent IL7R signalling would not suppress expression of the oncogenic IL7Rα and how mutant IL7Rα expression would affect conventional IL7Rα signalling, for example. In parallel to biochemical and cellular approaches, we suggest exploiting the power of mathematical and computational modelling, as presented in this review, to enhance our quantitative understanding of these complex immune signalling problems.

7 Discussion

This review is based on the hypothesis that the development of suitable mathematical models of immune signalling and receptor trafficking will allow us to provide answers to some current health-related challenges: how does the expression level (or its copy number) of a given protein in an immune receptor signalling pathway (or network) affect the type and timescale of cellular responses and how does ligand concentration or protein competition for binding sites on immune receptors drive different cellular fates by turning on/off different intra-cellular mechanisms, such as endocytosis, degradation, recycling or protein synthesis. From a mathematical perspective, the challenge is to develop a quantitative approach to how receptor-ligand signalling regulates cellular fate that (i) integrates a wide range of molecular, cellular and population data, and (ii) improves our understanding of the mechanisms that are dysregulated in disease, so that the mathematical models are accurate predictors of response to receptor-targeted therapies and can aid the design of novel drugs. In this regard, the ability to synthetically create ligands (referred to as *symthekines* [63]), with the ability to bring together receptor chains that are not naturally paired together, opens a door to novel ways to tune immune signalling. For instance, a dimeric compound of IL7 and IL15 (referred to as IL7.15 in Fig. 1), with the ability to bring together IL7Rα with IL15Rβ, can modulate IL7R and IL15R signalling, and thus T cell behaviour. Our belief is that mathematical modelling can help quantify, and even predict, the extent of this immune signalling modulation as a function of IL7 and IL15 extra-cellular concentration.

In the last decade a lot of quantitative work has supported the view that IL7 and its receptor, IL7R, are one of the master regulators of T cell homeostasis [19, 67]. Still a number of questions remain open, as discussed in this review. One of these challenges relates to intra-cellular events that take place once IL7R has been internalised. While much of the emphasis is often placed at the ligand-receptor level, trafficking, degradation, recycling and receptor synthesis are crucial to understanding how receptor-mediated signalling regulates immune cell fate. Thus, there is a need to develop mathematical models of immune signalling that incorporate receptor trafficking events [24, 62]. Recent

experimental advances [79] together with novel mathematical models will be essential to enhance our understanding of the mechanisms that regulate receptor-mediated immune signalling, and in turn will allow us to decipher how signalling determines immune cellular fate.
Finally, in this review we have presented a number of mathematical models, each of them at a different level of description (molecular, cellular and population, respectively). A current challenge and opportunity for applied mathematics is to integrate the different scales involved in the biological system under consideration. In this direction, agent-based models [80] are good candidates, as they bring together the characteristics of single cells with the dynamics of the whole population. Agent-based models, in combination with traditional mathematical models (based for instance in ODEs, as we discussed in Section 5.3), enable us to integrate different timescales.
We conclude with a reference to some recent work which has highlighted the relevance and significance of mathematical modelling in Immunology [81]. This latter reference has collected a number of studies of T cell immunology to illustrate the benefits of theoretical and experimental collaborations, not only at the receptor and signalling level, as we have done in this review.

Acknowledgements

This work has been supported by grants FIS2016-78883-C2-2-P and PRX 16/00287 (MC) from the Spanish Ministry of Economy (MINECO), the European Union FP7 Programme under agreement PIRSES-GA-2012-317893 (MC and CMP), and the European Union H2020 Programme under agreement 764698 MSCA-ITN-2017 (QuanTII ETN) (CMP).

References

[1] Peschon, JJ, *et al.* Journal of Experimental Medicine **180** (1994) 1955

[2] von Freeden-Jeffry, U, *et al.* Journal of Experimental Medicine **181** (1995) 1519

[3] Schluns, KS, *et al.* Nature immunology **1** (2000) 426

[4] Tan, JT, *et al.* Proceedings of the National Academy of Sciences **98** (2001) 8732

[5] Park, JH, *et al.* Nature immunology **11** (2010) 257

[6] Raeber, ME, *et al.* Immunological reviews **283** (2018) 176

[7] Kim, GY, *et al.* Immune network **11** (2011) 1

[8] Fry, TJ, *et al.* Blood **97** (2001) 2983

[9] Martin, CE, *et al.* Immunity **47** (2017) 171

[10] Waickman, AT, *et al.* Cellular and molecular life sciences **73** (2016) 253

[11] Rochman, Y, *et al.* Nature Reviews Immunology **9** (2009) 480

[12] Park, JH, *et al.* Immunity **21** (2004) 289

[13] Depper, JM, *et al.* Proceedings of the National Academy of Sciences **82** (1985) 4230

[14] Munitic, I, *et al.* Blood **104** (2004) 4165

[15] Kimura, MY, *et al.* Nature immunology **14** (2013) 143

[16] McElroy, CA, *et al.* Proceedings of the National Academy of Sciences **109** (2012) 2503

[17] Hong, C, *et al.* Immunity **40** (2014) 910

[18] Cotari, JW, *et al.* Science signaling **6** (2013) ra17

[19] Mazzucchelli, R, *et al.* Nature Reviews Immunology **7** (2007) 144

[20] Katz, G, *et al.* Sci Signal **7** (2014) ra83

[21] Callard, R, *et al.* Immunity **11** (1999) 507

[22] Palmer, MJ, *et al.* Cellular & molecular immunology **5** (2008) 79

[23] Feinerman, O, *et al.* Molecular systems biology **6** (2010) 437

[24] Reynolds, J, *et al.* Frontiers in immunology **4** (2013)

[25] Gonnord, P, *et al.* Sci Signal **11** (2018) eaal1253

[26] Yu, Q, *et al.* Journal of Experimental Medicine **203** (2006) 165

[27] McCaughtry, TM, *et al.* Journal of Experimental Medicine (2012) jem

[28] Park, JY, *et al.* Scientific reports **6** (2016)

[29] Kim, K, *et al.* The Journal of Immunology **160** (1998) 5735

[30] Yu, Q, *et al.* Journal of Experimental Medicine **200** (2004) 797

[31] Ligons, DL, *et al.* Journal of Biological Chemistry **287** (2012) 34386

[32] Marino, JH, *et al.* Human immunology **71** (2010) 329

[33] Singer, A, *et al.* Nature Reviews Immunology **8** (2008) 788

[34] Luckey, MA, *et al.* Nature immunology **15** (2014) 638

[35] Noguchi, M, *et al.* Proceedings of the National Academy of Sciences **94** (1997) 11534

[36] Chong, MM, *et al.* Immunity **18** (2003) 475

[37] Akashi, K, *et al.* Cell **89** (1997) 1033

[38] Opferman, JT, *et al.* Nature **426** (2003) 671

[39] Rathmell, JC, *et al.* The Journal of Immunology **167** (2001) 6869

[40] Yu, Q, *et al.* Journal of Experimental Medicine **197** (2003) 475

[41] Wofford, JA, *et al.* Blood **111** (2008) 2101

[42] Lee, HC, *et al.* The Journal of Immunology **174** (2005) 7800

[43] Kerdiles, YM, *et al.* Nature immunology **10** (2009) 176

[44] Feng, X, *et al.* Nature immunology **12** (2011) 544

[45] Abe, A, *et al.* The Journal of Immunology **195** (2015) 3129

[46] DeKoter, RP, *et al.* Immunity **16** (2002) 297

[47] Xue, HH, *et al.* Nature immunology **5** (2004) 1036

[48] Henriques, CM, *et al.* Blood **115** (2010) 3269

[49] Faller, EM, *et al.* Immunology and cell biology **94** (2016) 196

[50] Liu, W, *et al.* Journal of Experimental Medicine **203** (2006) 1701

[51] Jiang, Q, *et al.* Molecular and Cellular Biology **24** (2004) 6501

[52] Venkitaraman, AR, *et al.* European journal of immunology **24** (1994) 2168

[53] Noguchi, M, *et al.* Science **262** (1993) 1877

[54] Shimizu, A, *et al.* Immunological reviews **92** (1986) 103

[55] Walsh, ST. Immunological reviews **250** (2012) 303

[56] Fredriksson, S, *et al.* Nature biotechnology **20** (2002) 473

[57] Rose, T, *et al.* Journal of Biological Chemistry **285** (2010) 14898

[58] Palmer, MJ, *et al.* Immunology and cell biology **89** (2011) 581

[59] Waldmann, TA. Cancer immunology research **3** (2015) 219

[60] Fallon, EM, *et al.* Biotechnology progress **16** (2000) 905

[61] Busse, D, *et al.* Proceedings of the National Academy of Sciences **107** (2010) 3058

[62] de la Higuera, L, *et al.* In *Modeling Cellular Systems*, 81–105 (Springer, 2017)

[63] Moraga, I, *et al.* eLife **6** (2017) e22882

[64] Blinov, ML, *et al.* Bioinformatics **20** (2004) 3289

[65] Sekar, JA, *et al.* arXiv preprint arXiv:170906658 (2017)

[66] Faeder, JR, *et al.* Systems biology (2009) 113

[67] Takada, K, *et al.* Nature Reviews Immunology **9** (2009) 823

[68] Friedrich, C, *et al.* Immunity **47** (2017) 8

[69] Fry, TJ, *et al.* Blood **99** (2002) 3892

[70] Dooms, H. Journal of autoimmunity **45** (2013) 40

[71] Tal, N, *et al.* Cellular and molecular life sciences **71** (2014) 365

[72] Watanabe, M, *et al.* Journal of Experimental Medicine **187** (1998) 389

[73] Mazzucchelli, RI, *et al.* In *Seminars in immunology*, volume 24, 225–230 (Elsevier, 2012)

[74] Zenatti, PP, *et al.* Nature genetics **43** (2011) 932

[75] Kim, MS, *et al.* Human pathology **44** (2013) 551

[76] Ribeiro, D, *et al.* Advances in biological regulation **53** (2013) 211

[77] Shochat, C, *et al.* Blood **124** (2014) 106

[78] Durum, SK. Blood **124** (2014) 4

[79] Freed, DM, *et al.* Cell **171** (2017) 683

[80] Castro, M, *et al.* In *Stochastic Processes, Multiscale Modeling, and Numerical Methods for Computational Cellular Biology*, 127–140 (Springer, 2017)

[81] Castro, M, *et al.* Interface focus **6** (2016) 20150093

A Code listing for molecular level model (see Section 5.1)

```
begin model

begin parameters
NA 6.02214e23 # molecules per mol (Avogadro constant)
cellDensity 1e11 # cells per L (1e5 cells per uL)
Vecf=1/cellDensity
# concentration of IL-7 at time t=0
dens7 1 # nM (used for parametric plot)
IL7_0 dens7*1.0e-9*(NA*Vecf) # M converted to copies per cell (cpc)
# concentration of IL-15 at time t=0
dens15 0.10 # nM (used for parametric plot)
IL15_0 dens15*1.0e-9*(NA*Vecf) # M converted to copies per cell (cpc)
# number of receptors per cell
IL7Ralpha_0 1.0e3 # cpc
IL15Rbeta_0 1.0e3 # cpc
g0 1.0e3 # (used for parametric plot)
gammac_0 g0 # cpc
# Reaction rates (f: forward/ r: backward)
kf1 1.0e9/(NA*Vecf) # in units of M^{-1} min^{-1} converted to /(molecules/cell)/s
kr1 0.1 # in units of  min^{-1}
kf2 1.0e9/(NA*Vecf) # in units of M^{-1} min^{-1} converted to /(molecules/cell)/s
kr2 0.1 # in units of  min^{-1}
kf3 1.0e9/(NA*Vecf) # in units of M^{-1} min^{-1} converted to /(molecules/cell)/s
kr3 0.1 # in units of  min^{-1}
kf4 0.1*1.0e9/(NA*Vecf) # in units of M^{-1} min^{-1} converted to /(molecules/cell)/s
kr4 0.1 # in units of  min^{-1}
end parameters

begin molecule types
IL7(r,r) # IL-7 (ligand to be bound to receptor site "r" )
IL15(r,r) # IL-15 (ligand to be bound to receptor site "r")
IL7Ralpha(r,1) # IL-7Ralpha receptor (attach to gammac via "r" or ligand via "1")
IL15Rbeta(r,1) # IL-5Rbeta receptor (attach to gammac via "r" or ligand via "1")
gammac(r,1) # gammac (attach to gammac via "r" or ligand via "1")
end molecule types

begin seed species
IL7(r,r) IL7_0
IL15(r,r) IL15_0
IL7Ralpha(r,1) IL7Ralpha_0
IL15Rbeta(r,1) IL15Rbeta_0
gammac(r,1) gammac_0
end seed species

begin observables
Species Bound7R  IL7Ralpha.gammac.IL7
Species Bound15R  IL15Rbeta.gammac.IL15
end observables

begin functions
Fraction7() = Bound7R/(Bound7R+Bound15R)
end functions

begin reaction rules
IL7Ralpha(r,1) + gammac(r,1) <->IL7Ralpha(r!1,1).gammac(r!1,1) kf1,kr1 # heterodimerization
IL15Rbeta(r,1) + gammac(r,1) <->IL15Rbeta(r!1,1).gammac(r!1,1) kf2,kr2 # heterodimerization
# Binding
IL7Ralpha(r!1,1).gammac(r!1,1) + IL7(r,r) <->IL7Ralpha(r!1,1!2).gammac(r!1,1!3).IL7(r!2,r!3) kf3,kr3
IL15Rbeta(r!1,1).gammac(r!1,1) + IL15(r,r) <->IL15Rbeta(r!1,1!2).gammac(r!1,1!3).IL15(r!2,r!3) kf4,kr4
end reaction rules

end model

generate_network({overwrite=>1}); # Generate network
```

```
#simulate_ode({t_end=>1000, n_steps=>100,print_functions=>1}); # Get time-course
#parameter_scan({method=>"ode",par_min=>1e-1,par_max=>1e3,\
parameter_scan({method=>"ode",par_min=>1e0,par_max=>1e5,\
                n_scan_pts=>50,log_scale=>1,t_end=>1000,n_steps=>2,print_functions=>1,\
                parameter=>"dens7"}) # Change by dens15 or g0 for Figures 2b-c
```

B Code listing for population level stochastic model (see Section 5.3)

```
##########################################################################
# Simulation of IL-7 model using Gillespie algorithm and Euler method for
# solution of ODE governing IL-7 dynamics
##########################################################################

import numpy as np, matplotlib.pyplot as plt, math, random

I0 = 1
N1 = 50
N2 = 50
N3 = 50
N4 = 50

gam1 = 0.08
gam2 = 0.02
mu1 = 0.028
mu2 = 0.017
lam1 = 0.083
lam2 = 0.055
phi1 = 0.083
phi2 = 0.042

kap_s = 0.8
kap_p = 1.5
alpha = 5

h = 0.001
dt = 0.01
t_end = 300# 3350 # 72

delta = 0 # h^-1
nu = 50 # 1, 15, 50

n_steps = int(t_end / dt)

def IL7(n1,n2,n3,n4,I):
    return nu - gam1 * (n1 + n3) * I - gam2 * (n2 + n4) * I - delta * I

def rho_s(I):
    return 1 / (1 + math.exp(alpha * (I - kap_s)))

def rho_p(I):
    return 1 / (1 + math.exp(alpha * (kap_p - I)))

X = np.zeros((6,n_steps))

X[0][0] = I0
X[1][0] = N1
X[2][0] = N2
X[3][0] = N3
X[4][0] = N4
X[5][0] = N1+N2+N3+N4

I = I0
n1 = N1
n2 = N2
n3 = N3
n4 = N4
t = 0

IL=[]

for k in range(0,n_steps):
    while t < k*dt:
```

```
        if n1 == 0 and n2 == 0 and n3 == 0 and n4 == 0:
            break
        rmu1 = mu1*n1*rho_s(I)
        rmu2 = mu1*n2*rho_s(I)
        rmu3 = mu2*n3*rho_s(I)
        rmu4 = mu2*n4*rho_s(I)
        rlam1 = lam1*n1*rho_p(I)
        rlam2 = lam2*n3*rho_p(I)
        rphi1 = phi1*n2
        rphi2 = phi2*n4
        rtotal = rmu1+rmu2+rmu3+rmu4+rlam1+rlam2+rphi1+rphi2
        r1 = random.random()
        T = -(1/rtotal) * math.log(r1)
        t += T
        r2 = random.random()
        r2 = r2*rtotal

        if 0 <= r2 < rmu1:
            n1 -= 1
        elif rmu1 <= r2 < rmu1+rmu2:
            n2 -= 1
        elif rmu1+rmu2 <= r2 < rmu1+rmu2+rmu3:
            n3 -= 1
        elif rmu1+rmu2+rmu3 <= r2 < rmu1+rmu2+rmu3+rmu4:
            n4 -= 1
        elif rmu1+rmu2+rmu3+rmu4 <= r2 < rmu1+rmu2+rmu3+rmu4+rlam1:
            n1 -= 1
            n2 += 2
        elif rmu1+rmu2+rmu3+rmu4+rlam1 <= r2 < rmu1+rmu2+rmu3+rmu4+rlam1+rlam2:
            n3 -= 1
            n4 += 2
        elif rmu1+rmu2+rmu3+rmu4+rlam1+rlam2 <= r2 < rmu1+rmu2+rmu3+rmu4+rlam1+rlam2+rphi1:
            n1 += 1
            n2 -= 1
        elif rmu1+rmu2+rmu3+rmu4+rlam1+rlam2+rphi1 <= r2 < rtotal:
            n3 += 1
            n4 -= 1

        n_iter = int(T / h)
        for l in range(0,n_iter):
            I = I + h * IL7(n1,n2,n3,n4,I)
            IL.append(I)

    X[0][k] = I
    X[1][k] = n1
    X[2][k] = n2
    X[3][k] = n3
    X[4][k] = n4
    X[5][k] = n1+n2+n3+n4

xticks = []
tickinterval = t_end / (5*dt)
for k in range(0,6):
    xticks.append(k*tickinterval)
xlabels = []
ticks = t_end / 5
for k in range(0,6):
    xlabels.append(k*ticks)

Ixticks = []
Ixtickint = t_end / (5*h)
for k in range(0,6):
    Ixticks.append(k*Ixtickint)
Ilabels = []
Iticks = t_end / 5
for k in range(0,6):
    Ilabels.append(k*Iticks)
```

```
np.savetxt("concentration.csv",np.transpose(X), delimiter=" ")
np.savetxt("I.csv",np.transpose(IL), delimiter=" ")

fig = plt.figure()
plt.subplots_adjust(hspace=1.0)
ax1 = fig.add_subplot(132)
ax1.plot(X[1], label = 'CD5 High & IL-7R High', color = 'green')
ax1.plot(X[2], label = 'CD5 High & IL-7R Low', color = 'blue')
ax1.plot(X[3], label = 'CD5 Low & IL-7R High', color = 'red')
ax1.plot(X[4], label = 'CD5 Low & IL-7R Low', color = 'purple')
ax1.legend(bbox_to_anchor=(1.0, 1.0))
ax1.set_xlabel('Time (Hours)')
ax1.set_xticks(xticks)
ax1.set_xticklabels(xlabels)
ax1.set_ylabel('Cells')

ax3 = fig.add_subplot(133)
ax3.plot((X[1]+X[2])/X[5], label = 'CD5 High', color = 'blue')
ax3.plot((X[3]+X[4])/X[5], label = 'CD5 Low', color = 'red')
ax3.legend(bbox_to_anchor=(1.0, 1.0))
ax3.set_xlabel('Time (Hours)')
ax3.set_xticks(xticks)
ax3.set_xticklabels(xlabels)
ax3.set_ylabel('Cells')
ax3.set_ylim(0,1)

ax2 = fig.add_subplot(131)
ax2.plot(IL,color = 'blue')
ax2.set_xlabel('Time (Hours)')
ax2.set_xticks(Ixticks)
ax2.set_xticklabels(Ilabels)
ax2.set_ylabel('IL-7 Concentration')
plt.show()
```

C Code listing for population level deterministic model (see Section 5.3)

```
# Initial values:
#metabolites
init n12=50
init n22=50
init n21=50
init n11=50
init I=1

# Fixed Model Entities:
param mu1=0.028
param alpha=5
param kap_s=0.8
param mu2=0.017
param lam1=0.083
param kap_p=1.5
param lam2=0.055
param phi1=0.083
param phi2=0.042
param nu=15
param gam1=0.08
param gam2=0.02

# Assignment Model Entities:
n12_c=n12
n22_c=n22
I_c=I
n21_c=n21
n11_c=n11

#Kinetics:
Functio=mu1*n11_c/(1+exp(alpha*(I_c-kap_s)))
Functi=mu1*n12_c/(1+exp(alpha*(I_c-kap_s)))
Functi1=mu2*n21_c/(1+exp(alpha*(I_c-kap_s)))
Functi2=mu2*n22_c/(1+exp(alpha*(I_c-kap_s)))
Functi3=lam1*n11_c/(1+exp(alpha*(kap_p-I_c)))
Functi4=lam2*n21_c/(1+exp(alpha*(kap_p-I_c)))
Functi5=phi1*n12_c
Functi6=phi2*n22_c
Functi7=nu
Functi8=(gam1*(n11_c+n21_c)*I_c+gam2*(n12_c+n22_c)*I_c)

# Equations:
dn12/dt=-Functi+2*Functi3-Functi5
dn22/dt=-Functi2+2*Functi4-Functi6
dI/dt=Functi7-Functi8
dn21/dt=-Functi1-Functi4+Functi6
dn11/dt=-Functio-Functi3+Functi5
done
```